Electron scattering between *X* and *L* indirect valleys in type-I GaAs/AlAs semiconductor superlattices

M. Hosoda and J. Nohgi
Department of Applied Physics, Osaka City University, Sugimoto, Sumiyoshi-ku, Osaka 558-8585 Japan

N. Ohtani
Department of Electronics, Doshisha University, Tatara-Miyakodani, Kyotanabe, Kyoto 610-0321 Japan
(Received 14 February 2005; revised manuscript received 19 May 2005; published 21 July 2005)

We report evidence that an *X*-*L* transfer mechanism plays a significant role in carrier transport in semiconductor superlattices (SLs) under an electric field. Experimental observation of anomalously delayed photocurrent and photoluminescence from higher-energy subband states in a GaAs/AlAs type-I SL revealed that a switch of the electron transport path from Γ-X-Γ to Γ-X-L occurred by an electric field induced change of the subband alignment of the ground *X* state (X_1) in the barrier and the ground *L* state (L_1) in the adjacent well. The experimental results demonstrate that the electron scattering among the indirect valleys, i.e., the X_1 and L_1 subband states, is a significant transport channel in semiconductor SLs under high electric fields.

DOI: 10.1103/PhysRevB.72.033317 PACS number(s): 73.40.Kp, 72.80.Ey, 73.20.At, 73.50.Fq

The influence of indirect valleys, especially for *X* states, on electron transport in semiconductors is recognized in bulk GaAs as the Gunn effect.[1] However, in semiconductor superlattices (SLs), carriers cannot continue to flow in indirect states, because the bands are spatially and energetically separated by heterointerfaces. The effects of the *X* state in the barrier have been actively investigated for GaAs/AlAs type-II SLs, where photogenerated electrons in the quantum well (QW) Γ ground state (Γ_1) relax rapidly into the *X* state in the barrier and stay there.[2] On the contrary, in type-I SLs where the Γ state in the quantum well (QW) has a lower energy than the *X* state in the adjacent barrier, and where electron transport occurs by transitions between Γ states, the influence of the *X* state on carrier transport was not clearly identified until we clarified the function.[3–6]

Although electron scattering and wave-function mixing between direct Γ valley and indirect *X* or *L* valley states in bulk have been experimentally studied,[7–9] scattering and real-space transfer between indirect valley states have not been clarified because the influence of indirect states is difficult to observe experimentally, especially by luminescence. This is because indirect states cannot emit luminescence even when state mixing *between indirect states* occurs, since the *X* and *L* states have [100] and [111] momentum vectors, respectively; the mixing does not generate any [000] direct components. Although some experimental results for current-voltage characteristics have suggested electron scattering between indirect states, they do not clearly prove the states in which the electrons stay and flow. In addition, since *X* and *L* state energies are higher than the Γ ground state in many kinds of semiconductors, carrier occupation in the indirect valleys, which are the initial states for electron scattering toward the final indirect valley states, is difficult to establish due to relaxation. Consequently, electron transport from and to indirect states can hardly be observed experimentally. Thus, to date there have been no experimental reports to our knowledge on indirect-indirect scattering or on real-space transfer under resonance conditions between indirect states with different momentum vectors.

In this paper, we present evidence of carrier transport between *X* and *L* subband states in a type-I GaAs/AlAs SL. Experimental observation of anomalously delayed photocurrents in time-resolved photocurrent measurements and photoluminescence (PL) emission from higher-energy subband states indicates that *X*-*L* transport occurred between ground *X* state (X_1) in the barrier and ground *L* state (L_1) in the adjacent well under an electric field.

The sample structure used was a GaAs/AlAs type-I SL contained in a *p*-*i*-*n* diode grown on a (100)-oriented n^+-GaAs substrate by molecular beam epitaxy (MBE); the growth sequence is an n^+-GaAs layer, an *n*-$Al_{0.4}Ga_{0.6}As$ cladding layer, a nominally undoped 100-period GaAs/AlAs SL layer with a GaAs QW width of 18 monolayers (ML), and an AlAs barrier width of 16 ML, with 50 nm $Al_{0.4}Ga_{0.6}As$ undoped cladding layers on both sides, a *p*-$Al_{0.4}Ga_{0.6}As$ cladding layer, and a p^+-GaAs cap. The sample was fabricated into *p*-*i*-*n* diode mesas of 50 μm squares, which reduces the RC time constant to less than 100 ps. An 82 MHz repetition rate, 400 nm, 100-fs pulse width second harmonics light pulse of a Ti:sapphire laser, or 633 nm cw HeNe laser, were injected from the *p*-cap side. The time-resolved photocurrent was measured with a sampling oscilloscope. All experiments were done at 20 K.

Figure 1(a) shows the transition energy diagram of the sample between the electron subbands and the ground heavy-hole state (hh_1) in QW as a function of reverse bias voltage, which is calculated by a transfer matrix method using standard effective masses and energies.[10] The calculation contains a nonparabolicity effect on the Γ conduction band[11] and a quantum confined Stark effect (QCSE) on all the subband states as well as hh_1. Ordinarily, higher-energy hole states relax into the hh_1 state very rapidly, and forbidden transitions such as Γ_2-hh_1 transition under a zero electric field become allowed by the breaking symmetry of the wave functions under the QCSE regime. Therefore, we have shown only the electron transition energy between the hh_1 state, and evidently, only these transitions were observed experimentally.

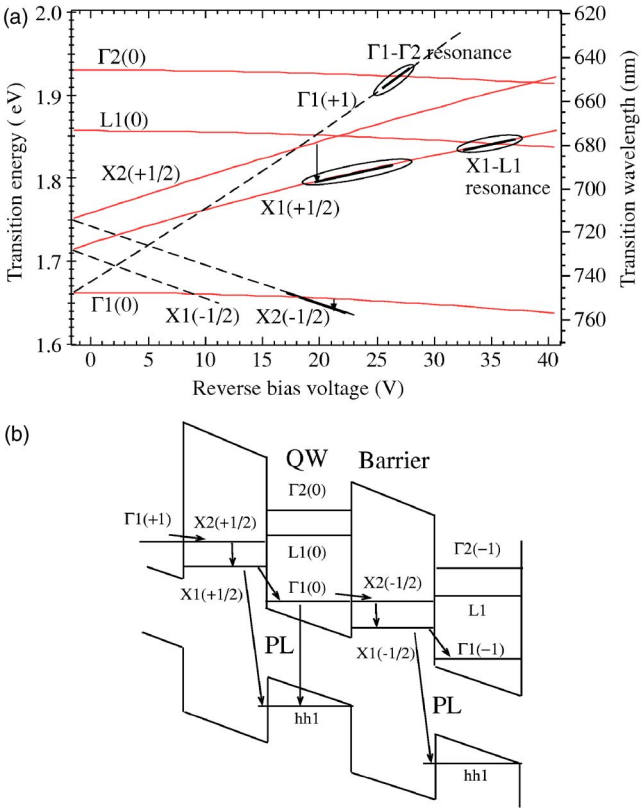

FIG. 1. (Color online) (a) Energy fancharts of calculated subbands as a function of reverse bias voltage at 20 K. The right vertical axis shows the PL wavelength corresponding to the transition energy. (b) Schematic energy diagram at 18 V.

Note that the X state treated in our present work results from the quantization of the X valley along the growth direction [001], i.e., the so-called X_z state, which considerably couples with the Γ state and a vertical real space transport. Because the probability density of the wave function, which leaks through remote barriers, is small in the sample barrier width, we only considered the first nearest-neighbor couplings. In this report, we omitted higher subband states and state crossings where the existence of carriers was not expected under the experimental conditions. The calculated Γ_n energies agreed well with the measured energies from PL spectra. We should note that resonances among hole states do not affect the experimental results, since higher-energy hole states relax into the hh_1 state very rapidly, and moreover, hole tunneling as well as resonances are weak due to the thick barrier of this SL. In addition, experiments for carrier transport observe only electron transport due to the very thin penetration depth of 400 nm excitation wavelength.

In the notations below, as shown in Fig. 1(b), the index in parentheses at each quantum state indicates the difference in period from a center base QW of 0 index, and the "+" and "−" signs indicate lower and higher energy states in the adjacent QW or barrier, respectively, compared to a center base QW under an applied electric field. A fractional index 1/2 denotes that the state is in a barrier, i.e., in a half period of the SL. These indices correspond to each Stark-ladder state. Note that $\Gamma_1(0)$-$X_1(-1/2)$ resonance and state crossing are

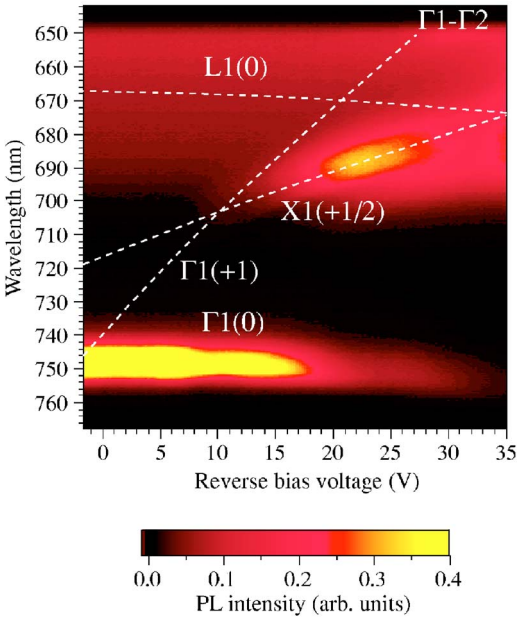

FIG. 2. (Color online) PL spectra under 4.5-mW HeNe laser irradiation as a function of reverse bias voltage. Brightness (false color) represents PL intensity. White dotted lines show calculated energies.

identical with $\Gamma_1(+1)$-$X_1(+1/2)$ and that the notation of the carrier transport depends only on the difference between indices of the energy states. Therefore, we use appropriate notations according to the situation in the following explanations.

Figure 2 shows the PL spectra of the sample for various reverse bias voltages. It is known that Γ state can resonate with the X states in SLs under an applied electric field, Γ-X scattering injects a number of electrons into the X state, and the X state can emit PL by Γ-X mixing.[4] Therefore, PL behavior in Fig. 2 is identified as follows: The slight quenching of Γ_1 PL around 9 V is considered an electron trap in the $X_1(-1/2)$ state by Γ_1-X_1 transport. The large decrease in Γ_1 PL intensity from 18 V indicates the reduction of Γ_1 occupation due to the trap of electrons by the $\Gamma_1(0)$-$X_2(-1/2)$ transfer. From the same voltage, electron transport to the X_1 state is greatly promoted through X_2-X_1 relaxation, which is supported by strong PL emission from the $X_1(+1/2)$ Stark-ladder PL. These energies and resonance voltages agree well with the fanchart in Fig. 1. PL at 650 nm is assigned PL from the Γ_2 state by Γ_1-Γ_2 resonant tunneling; its intensity is weak because of the 16 ML thick barrier width of the SL. The deviation of the Γ_1-Γ_2 resonance voltage at 27 V comes from electric field screening by high density carriers under 4.5-mW photoexcitation.

Figure 3 shows the precise PL spectra from higher energy subbands under weak photoexcitation. To show the weak PL region, logarithmic PL intensity (base=10) is displayed. Notice the two remarkable things. The first is the LO-phonon replica PL of the X_2 Stark-ladder state, which supports strong electron occupation into the X_2 state after Γ_1-X_2 resonance at 18 V, where X_2 state energy lowers Γ_1 state energy, effectively trapping electrons in the X_2 state. Then the electrons in

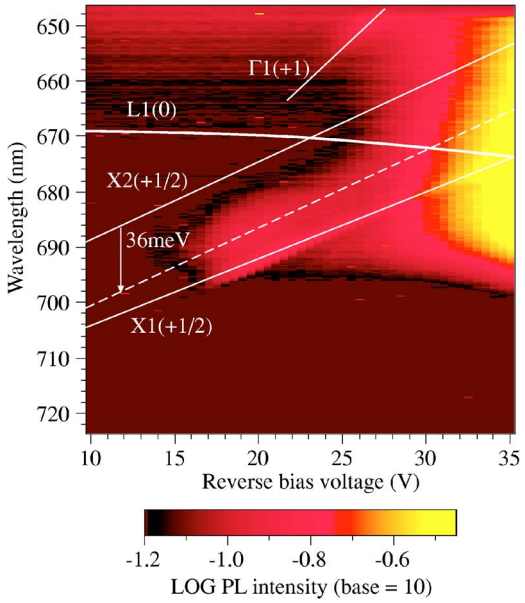

FIG. 3. (Color online) Precise PL spectra from higher energy states under 0.5-mW HeNe laser irradiation. Brightness (false color) represents logarithmic PL intensity.

the X_2 state relax to the X_1 state or relax with LO-phonon emission. Although Γ-X mixing is very weak due to large energy separation between the Γ and X states,[12] strong X_1 PL intensity indicates large electron occupation in the X_1 state that relaxed from the X_2 state. X_2-X_1 relaxation is most plausible due to the same momentum vectors. The second is that the PL has a broad emission spectrum at around 35 V, which is the PL from the hot electrons generated through the avalanche breakdown process.[5] This indicates the existence of a new carrier transport path open at 35 V, which releases trapped electrons in the X_1 state and greatly accelerates electron transport. This generates avalanche multiplication and hot electrons. Γ_1-Γ_2 resonant tunneling at 30 V is not a candidate for the new path, since the thick barrier inhibits tunneling, as supported by the very weak PL from the Γ_2 state. The PL from the indirect X_1 state is stronger than the direct Γ_2 state, which indicates that the electrons dominantly flow through the X_1 state, not the Γ_2 state.

Figure 4 shows the photocurrent versus reverse bias voltage characteristics (I-V curve) under 400-nm pulse laser excitation (the solid line). Figure 4 also shows the dark current of the sample (the dotted line). The dark current is in the order of picoamperes, which supports good sample quality. The increase from 20 V is interpreted as an escape of residual electrons existing in the SL even under the dark condition, through the Γ_1-X_2-X_1-L_1 channel with avalanche multiplication, which will be described later. Note that the photocurrent graph shows only electron transport characteristics because the penetration depth of the 400 nm wavelength is very shallow; thus only the electron charge sheet runs through the SL. We should also note that a different I-V curve was observed under HeNe laser excitation which contains the influence of the hole transport. From the I-V curve, electron transport reaches a plateau approximately after the Γ_1-X_1 resonance, indicating less efficient Γ_1-Γ_1 nonresonant

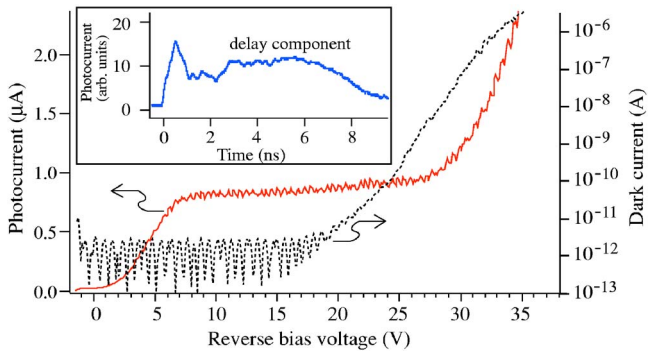

FIG. 4. (Color online) Solid line: Time integrated photocurrent versus reverse bias voltage under 0.1-mW 400-nm Ti:sapphire pulse laser excitation. Dotted line: Dark current. Inset: photocurrent impulse response at 20 V, which has a delay component.

sequential tunneling in the SL due to a thick barrier. Electron transport is greatly increased from about 30 V, and finally the SL shows avalanche breakdown at around 35 V. This indicates that a new carrier transport path has opened at around 35 V.

Figure 5 shows the bias voltage dependence of the time-resolved photocurrent response [Pc(t)], that is the time-resolved I-V characteristics (TIV graph) composed from Pc(t) at each bias voltage as shown in the Fig. 4 inset. Pc(t) at voltages greater than 9 V shows a delay component that reduces delay by increasing bias voltage, and it finally converges to a fast single Pc(t) peak at 35 V. The anomalously delayed components originated from the trapped electrons in the X states.[6] While Pc(t) shows a delay component, the I-V curve in Fig. 4 has a flat plateau in the region from about 8 to 28 V. This supports the fact that most of the photoelectrons are swept out in a long time range. From 9 V, once an elec-

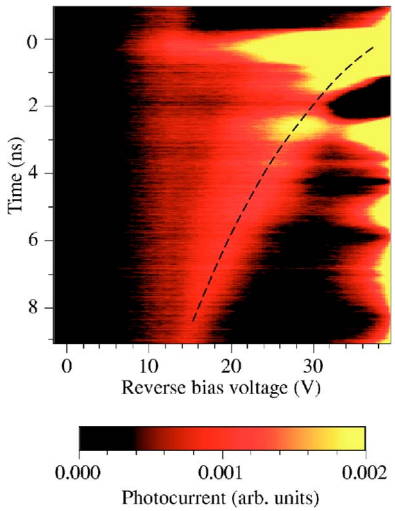

FIG. 5. (Color online) Time-resolved photocurrent response image (TIV graph). Brightness (false color) represents photocurrent intensity. "Time=0" denotes the starting time of optical pulse excitation. Weak horizontal lines at 2.8 and 5.5 ns and periodical peaks at 37-40 V are spurious ringing signals caused by an impedance mismatch of circuits. The dashed line indicates hastening of the delay components.

tron is captured from the Γ_1 state into a type-II aligned X_1 state in the barriers, the electron will remain there for the relatively long relaxation time of the X_1-Γ_1.[2] Slow relaxation, i.e., the trap function of the X state, originates from the large density of state of the X state.[2] In this case, Pc(t) will have a weak and slow tail, as exemplified by the Pc(t) in the Fig. 4 inset. The shortening of the delay comes from the opening of a new escape channel from the X_1 state, which we first found in SLs having an X_1-Γ_2 escape path.[6] In contrast to the previous reported SLs having energetically lower Γ_2 states than L_1 states in the adjacent QW, the energy level of the L_1 state in the present SL is lower than the Γ_2 state, as shown in Figs. 1–3. Therefore, the new escape path must be the X_1-L_1 transfer.

The experimental results described so far can be interpreted as follows: The trapping of the electrons in the X_1 state starts by the Γ_1-X_1 transfer from 9 V (cf. Figs. 2 and 5) and is enhanced by the Γ_1-X_2-X_1 transfer from 18 V (cf. Figs. 2 and 3). This scheme is shown in Fig. 1(b). Once the X_1-L_1 path is opened, the electrons can escape from the X_1 state and effectively flow through the SL via the L state (cf. Figs. 3–5). Figure 6 shows this scheme. To confirm the hypothesis, other GaAs/AlAs superlattice samples having similar energy structure, that is, X_1 meets L_1 before Γ_2, were also grown by other molecular beam epitaxy (MBE) systems, and measured. A similar phenomenon was observed.

The experimental results extracted additional information on X-L scattering. The X_1-L_1 transfer time is estimated to be equal or less than a picosecond by evaluating approximately one nanosecond pulse width of Pc(t) at 35 V, where the electron charge sheet runs through the 100 periods of the SL by X_1-L_1 transfer with other relaxation processes. Since the measured voltage of the X_1-L_1 resonance agrees with the calculated value and has no deviation corresponding to the LO-phonon energy, X-L scattering is thought to originate from the interface roughness.

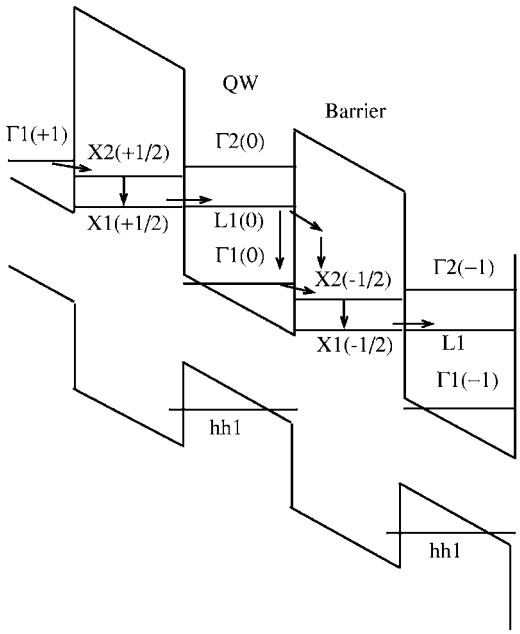

FIG. 6. Schematic diagrams of X_1-L_1 transfer.

In conclusion, we have found an X-L intersubband transport in a SL. After electrons occupy the X_1 state in the barrier and when the L state energy level in the adjacent QW is closer than the other subband states under an electric field, X-L scattering and transfer occur very effectively. The above SL structure may assist future investigations on carrier scattering and transport between indirect valleys having different momentum vectors.

A part of this study was supported by a Grant-in-Aid (No. 14350013) from the Ministry of Education, Culture, Sports, Science, and Technology of Japan.

[1] J. B. Gunn, Solid State Commun. **1**, 88 (1963).
[2] For example, see J. Feldmann and E. L. Göbel, in *Optics of Semiconductor NanoStructures*, edited by F. Henneberger, S. Schmitt-Rink, and E. O. Göbel (Akademie Verlag, Berlin, 1993), Chap. I-7, and references therein.
[3] M. Hosoda, N. Ohtani, H. Mimura, K. Tominaga, P. Davis, T. Watanabe, G. Tanaka, and K. Fujiwara, Phys. Rev. Lett. **75**, 4500 (1995).
[4] M. Hosoda, H. Mimura, N. Ohtani, K. Tominaga, K. Fujita, T. Watanabe, H. Inomata, and M. Nakayama, Phys. Rev. B **55**, 13689 (1997).
[5] M. Hosoda, K. Tominaga, N. Ohtani, K. Kuroyanagi, N. Egami, H. Mimura, K. Kawashima, and K. Fujiwara, Appl. Phys. Lett. **71**, 2827 (1997).
[6] M. Hosoda, N. Ohtani, H. Mimura, K. Tominaga, T. Watanabe, H. Inomata, and K. Fujiwara, Phys. Rev. B **58**, 7166 (1998).
[7] R. G. Ulbrich, J. A. Kash, and J. C. Tsang, Phys. Rev. Lett. **62**, 949 (1989).
[8] J. W. Cockburn, J. J. Finley, P. Wisniewski, M. S. Skolnick, R. Teissier, D. J. Mowbray, R. Grey, G. Hill, and M. A. Pate, Phys. Rev. B **54**, 4472 (1996).
[9] D. Rakoczy, G. Strasser, C. Strahberger, and J. Smoliner, Phys. Rev. B **66**, 033309 (2002).
[10] S. Adachi, J. Appl. Phys. **58**, R1 (1985).
[11] D. F. Nelson, R. C. Miller, and D. A. Kleinman, Phys. Rev. B **35**, R7770 (1987).
[12] M. Nakayama, K. Imazawa, K. Suyama, I. Tanaka, and H. Nishimura, Phys. Rev. B **49**, 13564 (1994).